# Strange form factors on the lattice

Jeremy Green

Institut für Kernphysik, Johannes Gutenberg-Universität Mainz

Intersections of BSM Phenomenology
and QCD for New Physics Searches
Institute for Nuclear Theory
September 14–October 23, 2015

# Nucleons

The *net* quark content of a proton is *uud* and of a neutron is *ddu*.

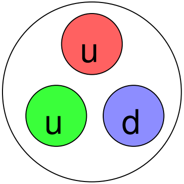


But quantum fluctuations can produce gluons and $\bar{q}q$ pairs, including also heavier quarks ($s$, ...).

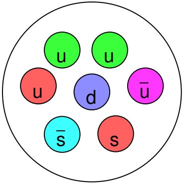

# Electromagnetic form factors

We can probe the structure of a proton using virtual photons, which couple to quarks via the current

$$J_\mu^\gamma = \tfrac{2}{3}\bar{u}\gamma_\mu u - \tfrac{1}{3}\bar{d}\gamma_\mu d - \tfrac{1}{3}\bar{s}\gamma_\mu s + \ldots$$

Symmetries constrain matrix elements between proton states with momenta $p$ and $p'$:

$$\langle p'|J_\mu^\gamma|p\rangle = \bar{u}(p')\left[\gamma_\mu F_1^\gamma(Q^2) + \tfrac{i\sigma_{\mu\nu}(p'-p)^\nu}{2m_p} F_2^\gamma(Q^2)\right] u(p),$$

where $Q^2 = -(p'-p)^2$ is the four-momentum transfer and $F_{1,2}^\gamma$ are the Dirac and Pauli form factors.
Electric and magnetic form factors:

$$G_E^\gamma(Q^2) = F_1^\gamma(Q^2) - \tfrac{Q^2}{(2m_p)^2} F_2^\gamma(Q^2), \qquad G_M^\gamma(Q^2) = F_1^\gamma(Q^2) + F_2^\gamma(Q^2)$$

# Electromagnetic form factors

In the *nonrelativistic limit*, $G_E(Q^2)$ and $G_M(Q^2)$ are Fourier transforms of the charge and magnetization densities in a proton.

- $G_E^\gamma(0) = 1$, the charge of a proton
- $G_M^\gamma(0) = \mu$, the magnetic moment of a proton, in units of the nuclear magneton $\mu_N = \frac{e}{2m_p}$

Even though this interpretation doesn't hold relativistically, it is still used to *define* the charge and magnetic radii using the derivatives at $Q^2 = 0$:

- $r_E^2 = -6G_E^{\gamma\,\prime}(0)$
- $r_M^2 = -6G_M^{\gamma\,\prime}(0)/\mu$

Relativistically, there is a rigorous interpretation of $F_1(Q^2)$ as the 2-D Fourier transform of the transverse charge density in the infinite-momentum frame.

# Elastic *ep* scattering

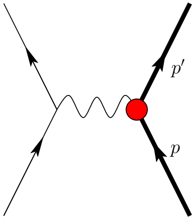


Elastic scattering of an electron off a fixed proton target has a leading contribution from single photon exchange,

which contributes to the cross section

$$\sigma \propto G_E^\gamma(Q^2)^2 + \frac{\tau}{\epsilon} G_M^\gamma(Q^2)^2, \qquad \tau = \frac{Q^2}{4m_p^2}, \quad \epsilon^{-1} = 1 + 2(2+\tau)\tan^2\tfrac{\theta}{2},$$

thus allowing the form factors to be measured in experiments.

# Aside: radius from spectroscopy

Spectroscopy is also sensitive to the proton $r_E$.

In a hydrogen atom, the S orbitals have the proton located at an antinode of the electron's wavefunction, whereas the P orbitals have it located at a node.

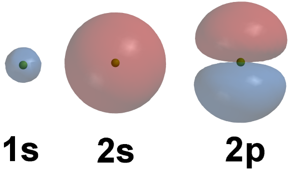


Thus the 2S–2P Lamb shift is sensitive to the finite radius of the proton.

If the electron is replaced by a muon (200× heavier), the orbitals will be smaller and the effect becomes bigger (2% of the Lamb shift).

# Aside: proton radius problem


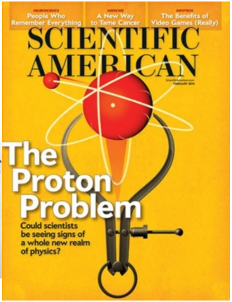


$7\sigma$ discrepancy between results from Lamb shift and muonic hydrogen and combined results from electron-proton scattering+spectroscopy.

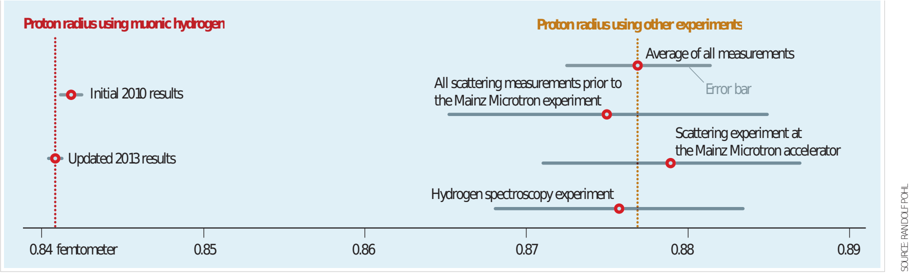


(J. C. Bernauer and R. Pohl, Scientific American, February 2014)

# Flavour separation

Form factors of a neutron are measured in experiments using scattering of $^2$H or $^3$He targets. Using approximate *charge symmetry*, which says that:

- a $u$ quark in a proton ($uud$) behaves like a $d$ quark in a neutron ($ddu$)
- a $d$ quark in a proton ($uud$) behaves like a $u$ quark in a neutron ($ddu$)

then we have

$$
\begin{aligned}
G_{E,M}^{\gamma(p)} &= \tfrac{2}{3} G_{E,M}^{u} - \tfrac{1}{3} G_{E,M}^{d} + \dots \\
G_{E,M}^{\gamma(n)} &= \tfrac{2}{3} G_{E,M}^{d} - \tfrac{1}{3} G_{E,M}^{u} + \dots
\end{aligned}
$$

Neglecting heavier quarks allows the $u$ and $d$ form factors to be isolated.

# Measuring strange form factors

Using a single probe (photons) and two targets (protons and neutrons) allows for isolating two flavour contributions.
To isolate the next-largest contribution, from $s$ quarks, use a different probe: $Z$ bosons.

$$J_\mu^{ZV} = (1 - \tfrac{8}{3}\sin^2\theta_W)\bar{u}\gamma_\mu u - (1 - \tfrac{4}{3}\sin^2\theta_W)(\bar{d}\gamma_\mu d + \bar{s}\gamma_\mu s) + \dots$$

By measuring the parity-violating asymmetry in elastic $\vec{e}p$ scattering,

$$A_{LR} = \frac{\sigma_R - \sigma_L}{\sigma_R + \sigma_L},$$

the leading single-photon-exchange contribution can be eliminated and the interference between $\gamma$ and $Z$ exchange diagrams can be isolated.

# Experiments at forward scattering angles

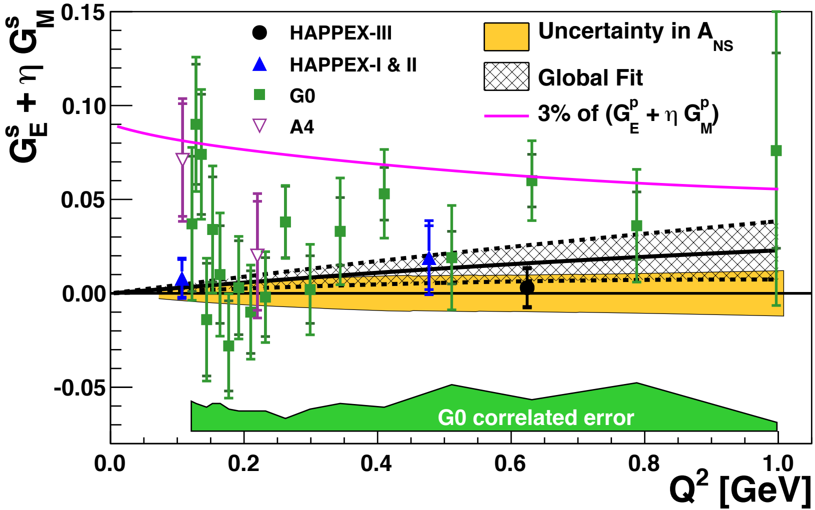


$\eta \approx AQ^2$, $A = 0.94\ \text{GeV}^{-2}$

(HAPPEX Collaboration, Phys. Rev. Lett. **108** (2012) 102001 [1107.0913])

# $G_E^s$ and $G_M^s$ at $Q^2 \approx 0.62\ \mathrm{GeV}^2$

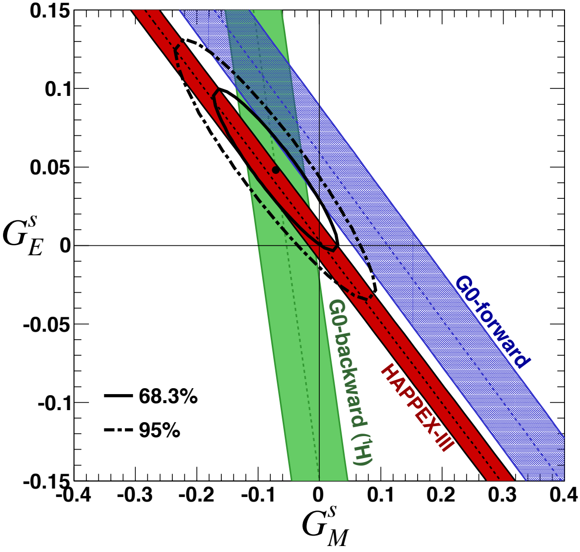


(HAPPEX Collaboration, Phys. Rev. Lett. **108** (2012) 102001 [1107.0913])

# Lattice QCD

…is a regularization of Euclidean-space QCD such that the path integral can be done fully non-perturbatively

- Euclidean spacetime becomes a periodic hypercubic lattice, with spacing $a$ and box size $L_s^3 \times L_t$.
- Path integral over fermion degrees of freedom is done analytically, for each gauge configuration. Solving the Dirac equation with a fixed source yields a source-to-all quark propagator.
- Path integral over gauge degrees of freedom is done numerically using Monte Carlo methods to generate an *ensemble* of *gauge configurations*.

The $a \to 0$ and $L_s, L_t \to \infty$ extrapolations need to be taken by using multiple ensembles.

# Nucleon matrix elements using lattice QCD

To find matrix elements, compute

$$C_{2\text{pt}}(t,\vec{p}) = \sum_{\vec{x}} e^{-i\vec{p}\cdot\vec{x}} \langle N(\vec{x},t)\bar{N}(\vec{0},0)\rangle$$

$$\xrightarrow{t\to\infty} e^{-E(\vec{p})t} |\langle p|\bar{N}|\Omega\rangle|^2$$

$$C_{3\text{pt}}(T,\tau;\vec{p},\vec{p}\,') = \sum_{\vec{x},\vec{y}} e^{-i\vec{p}\,'\cdot\vec{x}} e^{i(\vec{p}\,'-\vec{p})\cdot\vec{y}} \langle N(\vec{x},T)\mathcal{O}(\vec{y},\tau)\bar{N}(\vec{0},0)\rangle$$

$$\xrightarrow[T-\tau\to\infty]{\tau\to\infty} e^{-E(\vec{p}\,')(T-\tau)} e^{-E(\vec{p})\tau} \langle\Omega|N|p'\rangle\langle p'|\mathcal{O}|p\rangle\langle p|\bar{N}|\Omega\rangle$$

Then form ratios to isolate $\langle p'|\mathcal{O}|p\rangle$.
For $\mathcal{O}$ a quark bilinear, there are two kinds of quark contractions for $C_{3\text{pt}}$:

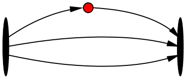

*connected*

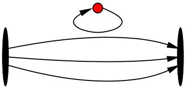

*disconnected*

# Connected contractions

We have efficient solvers for source-to-all quark propagators. Connected contractions can be computed using these via the *sequential propagator* technique.

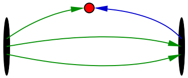

1. Fix the source and compute the forward propagator.
2. Fix the sink and $T$; compute the backward (sequential) propagator.
3. Combine the two to compute arbitrary $\mathcal{O} = \bar{q} \dots q$, for all $\tau \in [0, T]$.

For the proton, these contribute for $q \in \{u, d\}$. If we take isovector ($u - d$) observables, then these are the only contributing contractions.

# Disconnected contractions

For strange quarks in the proton, these are the only contribution.
Disconneced light quarks are also needed for, e.g., the proton radius.

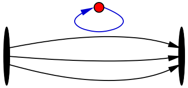

Using, e.g., $\mathcal{O} = \bar{q}\Gamma q$, these involve the disconnected loop,

$$T(\vec{q}, t, \Gamma) = -\sum_{\vec{x}} e^{i\vec{q}\cdot\vec{x}} \operatorname{Tr}[\Gamma D^{-1}(x, x)],$$

which involves the quark propagator $D^{-1}(x, y)$ from every point on a timeslice back to itself.

We can estimate the all-to-all propagator stochastically using noise sources $\eta$ that satisfy $E(\eta\eta^\dagger) = I$. By solving $\psi = D^{-1}\eta$, we get

$$D^{-1}(x, y) = E(\psi(x)\eta^\dagger(y)).$$

# Dilution

For a random vector $\eta$ with components of magnitude $|\eta_i| = 1$, the diagonal of $\eta\eta^\dagger$ is exact and the variance comes from the off-diagonal parts.

$$\text{e.g.} \quad \eta = \begin{pmatrix} \eta_1 \\ \eta_2 \\ \eta_3 \\ \eta_4 \end{pmatrix}, \quad \eta\eta^\dagger = \begin{pmatrix} 1 & \eta_1\eta_2^* & \eta_1\eta_3^* & \eta_1\eta_4^* \\ \eta_2\eta_1^* & 1 & \eta_2\eta_3^* & \eta_2\eta_4^* \\ \eta_3\eta_1^* & \eta_3\eta_2^* & 1 & \eta_3\eta_4^* \\ \eta_4\eta_1^* & \eta_4\eta_2^* & \eta_4\eta_3^* & 1 \end{pmatrix}, \quad E(\eta\eta^\dagger) = I$$

*Dilution*: use a complete set of projectors $\{P_b | P_b^2 = P_b, \sum_b P_b = I\}$ to partition the components of $\eta$ and eliminate parts of the variance:

$$\eta^{(b)} \equiv P_b \eta; \qquad E\left(\sum_b \eta^{(b)}\eta^{(b)\dagger}\right) = I$$

$$\text{e.g.} \quad \eta^{(1)} = \begin{pmatrix} \eta_1 \\ \eta_2 \\ 0 \\ 0 \end{pmatrix}, \eta^{(2)} = \begin{pmatrix} 0 \\ 0 \\ \eta_3 \\ \eta_4 \end{pmatrix}, \quad \sum_b \eta^{(b)}\eta^{(b)\dagger} = \begin{pmatrix} 1 & \eta_1\eta_2^* & 0 & 0 \\ \eta_2\eta_1^* & 1 & 0 & 0 \\ 0 & 0 & 1 & \eta_3\eta_4^* \\ 0 & 0 & \eta_4\eta_3^* & 1 \end{pmatrix}$$

# Dilution

In many cases, using $N$ dilution projectors to target the most important parts of the noise yields a better than $1/\sqrt{N}$ reduction. Commonly used:

- Spin dilution
- Colour dilution
- Spatial dilution

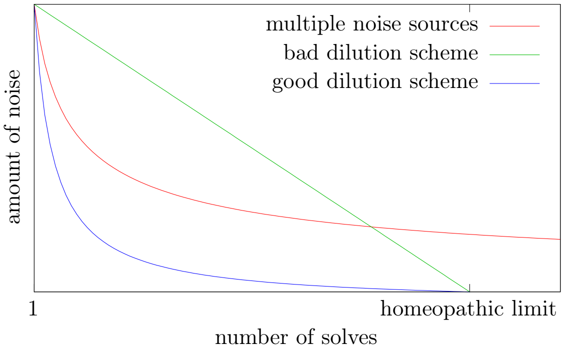


In the *homeopathic limit*, complete dilution is equivalent to fully computing a disconnected loop without stochastic estimation.

# Hadamard vectors

*Hadamard vectors* $h_b$ can be used to obtain the same results as dilution, by taking the component-wise product $\eta^{[b]} \equiv h_b \odot \eta$ and averaging over $b$.
e.g. Hadamard vectors: $h_1 = (1,1,1,1)$, $h_2 = (1,1,-1,-1)$

$$\eta^{[1]} = \begin{pmatrix} \eta_1 \\ \eta_2 \\ \eta_3 \\ \eta_4 \end{pmatrix}, \eta^{[2]} = \begin{pmatrix} \eta_1 \\ \eta_2 \\ -\eta_3 \\ -\eta_4 \end{pmatrix}, \quad \frac{1}{2}\sum_b \eta^{[b]}\eta^{[b]\dagger} = \begin{pmatrix} 1 & \eta_1\eta_2^* & 0 & 0 \\ \eta_2\eta_1^* & 1 & 0 & 0 \\ 0 & 0 & 1 & \eta_3\eta_4^* \\ 0 & 0 & \eta_4\eta_3^* & 1 \end{pmatrix}$$

If we had used only $\eta^{[1]}$, we would also get the correct expectation value (only with more noise).
$\longrightarrow$ Hadamard vectors allow for progressively increasing the level of dilution, while making use of previous effort.

# Hierarchical probing

(A. Stathopoulos, J. Laeuchli, K. Orginos, SIAM J. Sci. Comput. **35(5)** (2013) S299–S322 [1302.4018])

Use a sequence of specially-constructed spatial Hadamard vectors in order to progressively increase the level of spatial dilution.

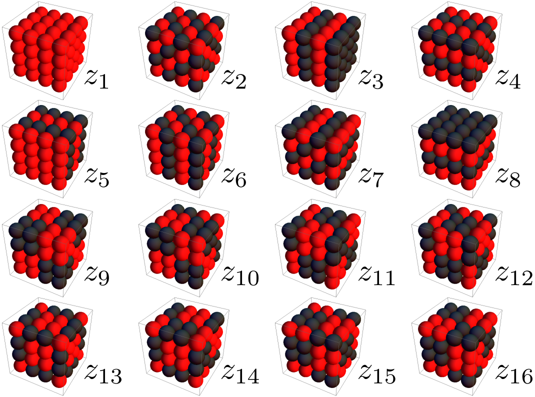


red: $+1$
black: $-1$

We use 128 three-dimensional Hadamard vectors to eliminate the variance from neighboring sites up to distance 4.

# Lattice calculation

RAPID COMMUNICATIONS

PHYSICAL REVIEW D **92,** 031501(R) (2015)

**High-precision calculation of the strange nucleon electromagnetic form factors**

Jeremy Green,[1,*] Stefan Meinel,[2,3,†] Michael Engelhardt,[4] Stefan Krieg,[5,6] Jesse Laeuchli,[7] John Negele,[8] Kostas Orginos,[9,10] Andrew Pochinsky,[8] and Sergey Syritsyn[3]

[arXiv: 1505.01803]

- $N_f = 2 + 1$ Wilson-clover fermions
- $a = 0.114$ fm, $32^3 \times 96$
- $m_u = m_d > m_{ud}^{\text{phys}}$, corresponding to pion mass 317 MeV
- $m_s \approx m_s^{\text{phys}}$
- 1028 gauge configurations
- disconnected loops for six source timeslices (128 Hadamard vectors, plus color+spin dilution)
- two-point correlators from 96 source positions

# Hierarchical probing vs. many noise sources

Study using 1/3 of gauge configurations.

$G_M^{(\frac{2}{3}u-\frac{1}{3}d)}$ $(Q^2 \approx 0.11\ \text{GeV}^2)$ (disconnected)

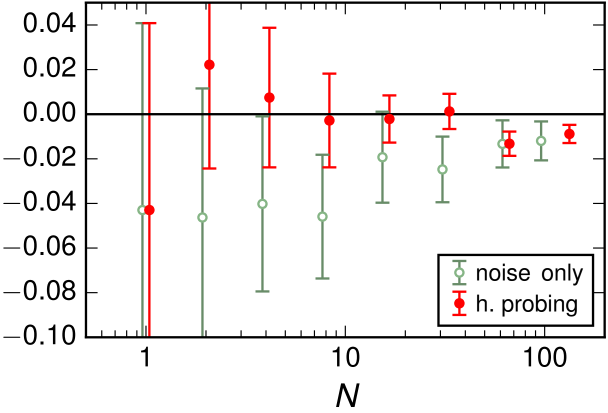


Equal cost at same $N$ ($= N_{\text{Hadamard}}$ or $N_{\text{noise}}$).

Points offset horizontally.

(S. Meinel, Lattice 2014)

# Disconnected $G_E(Q^2)$

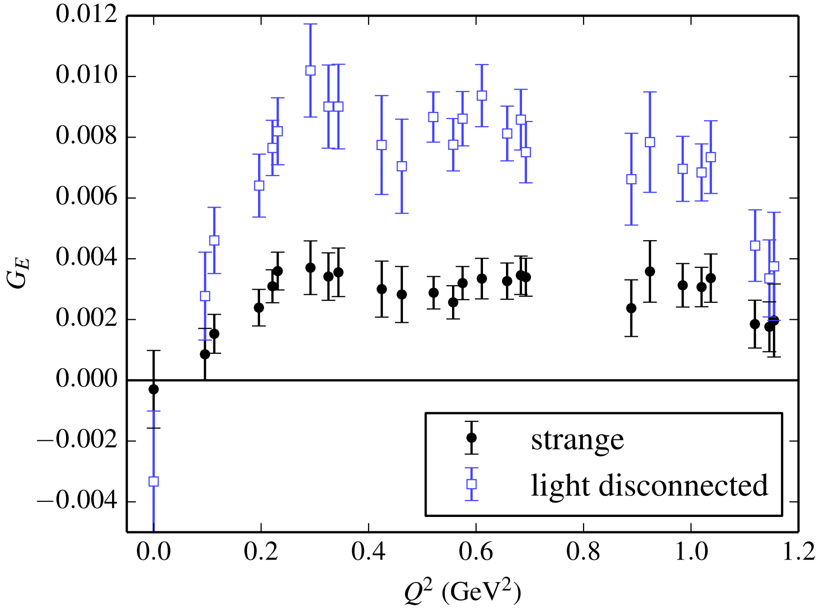

# Disconnected $G_M(Q^2)$

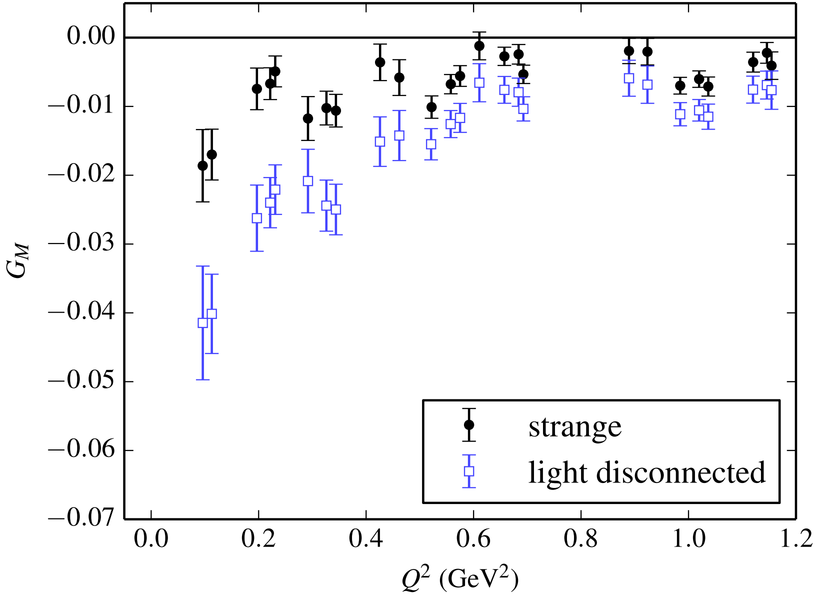

# Fitting $Q^2$-dependence

We want to fit $G_{E,M}(Q^2)$ with curves to determine the radii and magnetic moment from the slope and intercept at $Q^2 = 0$.

- Common approach: use simple fit forms such as a dipole.
- Better: use $z$-expansion. Conformally map domain where $G(Q^2)$ is analytic in complex $Q^2$ to $|z| < 1$, then use a Taylor series:

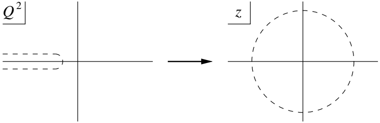


[R. J. Hill and G. Paz, Phys. Rev. D **82** (2010) 113005]

$$z(Q^2) = \frac{\sqrt{t_\text{cut} + Q^2} - \sqrt{t_\text{cut}}}{\sqrt{t_\text{cut} + Q^2} + \sqrt{t_\text{cut}}},$$

$$G(Q^2) = \sum_k a_k z(Q^2)^k,$$

with Gaussian priors imposed on the coefficients $a_k$. Specifically,

- For $G_E$, set $a_0 = 0$ (charge conservation) and leave $a_1$ unconstrained.
- For $G_M$, leave $a_0$ and $a_1$ unconstrained.

Thus $r_{E,M}$ and $\mu$ are not directly constrained.

For higher coefficients, impose $|a_{k>1}| < 5 \max\{|a_0|, |a_1|\}$, and vary the bound to estimate systematic uncertainty.

# Disconnected $G_E(Q^2)$

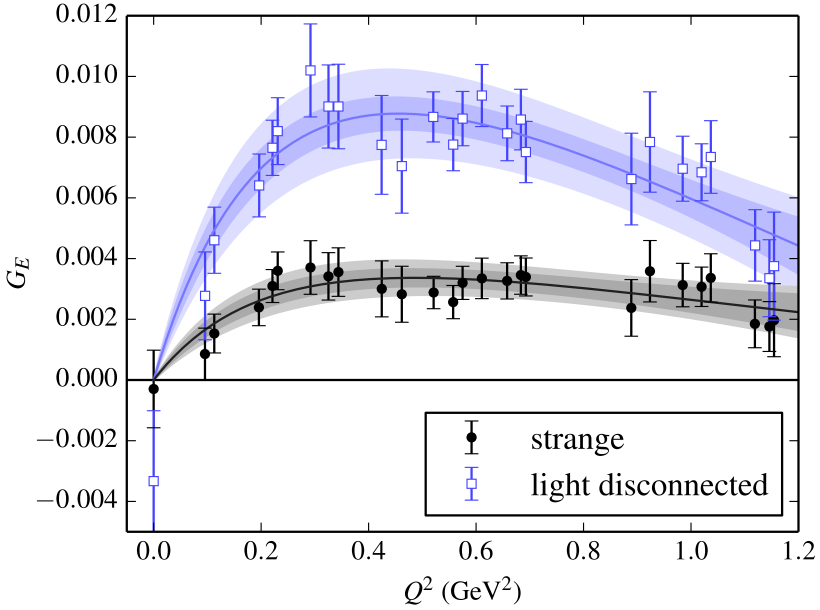

# Disconnected $G_M(Q^2)$

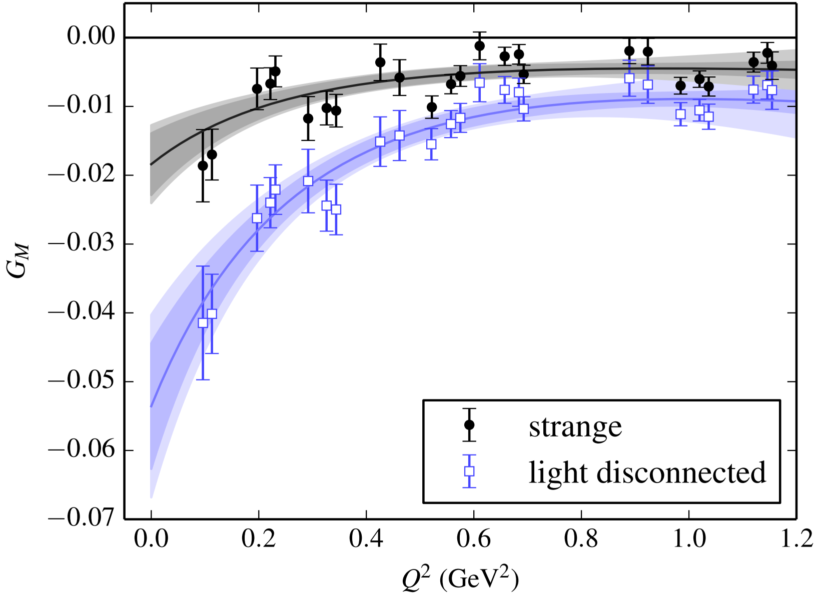

# Strange magnetic moment and radii at $m_\pi = 317$ MeV

For the unphysical quark masses used on this ensemble:

$$(r_E^2)^s = -0.0054(9)(6)(11)(2)\ \mathrm{fm}^2,$$
$$(r_M^2)^s = -0.0147(61)(28)(34)(5)\ \mathrm{fm}^2,$$
$$\mu^s = -0.0184(45)(12)(32)(1)\ \mu_N^{\mathrm{lat}},$$

where the uncertainties are

1. statistical
2. fitting
3. excited states
4. discretization

Finite-volume effects neglected since $m_\pi L = 5.9$.

# Extrapolation to the physical point

We would like to extrapolate from unphysical quark masses using chiral perturbation theory (ChPT).
For $u$, $d$, and $s$ quarks, and nucleons, we need $SU(3)$ heavy baryon ChPT.

- degrees of freedom: meson octet ($\pi$, $K$, $\eta$) and baryon octet ($N$, $\Sigma$, $\Lambda$, $\Xi$)
- known parameters: meson decay constant $f$, baryon axial couplings $F$, $D$

At leading one-loop order:

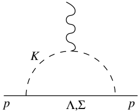


$$(r_E^2)^s = \frac{1}{16\pi^2 f^2}\left(c_1(\mu) + \frac{9+5c_{DF}}{3}\log\frac{m_K}{\mu}\right),$$

$$\mu^s = c_2 + \frac{m_p m_K}{24\pi f^2} c_{DF},$$

$$(r_M^2)^s = -\frac{m_p}{48\pi f^2 m_K} c_{DF},$$

[M. Musolf, H. Ito, Phys. Rev. C **55** (1997) 3066
T. R. Hemmert *et al.*, Phys. Lett. B **437** (1998) 184
T. R. Hemmert *et al.*, Phys. Rev. C **60** (1999) 045501]

where $c_1(\mu)$ and $c_2$ are unknown parameters, and $c_{DF} = 5D^2 - 6DF + 9F^2$.

# Disconnected light-quark observables in ChPT

By themselves, the disconnected light-quark form factors are unphysical, but they can be understood in partially quenched QCD and partially quenched ChPT: $q \in \{u, d, s\} \to q \in \{u, d, s, l, \tilde{l}\}$.
At leading one-loop order, one can simply modify the mass of the strange quark in the loop, i.e., replace $m_K$ with $m_{\text{loop}}$, where

$$m_{\text{loop}} = \begin{cases} m_K & \text{for strange quarks} \\ m_\pi & \text{for disconnected light quarks} \end{cases}$$

Thus with the leading one-loop formulas we can interpolate to the physical kaon mass.

# Partially quenched ChPT at leading one-loop order

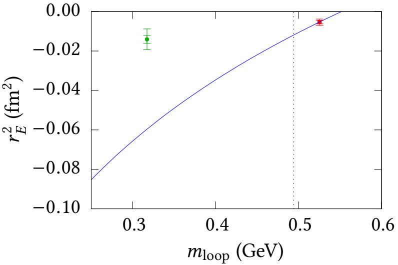


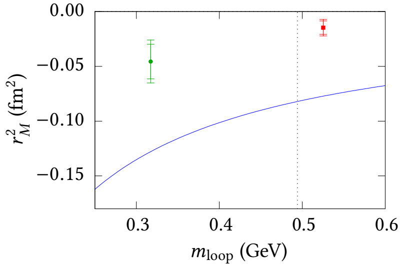


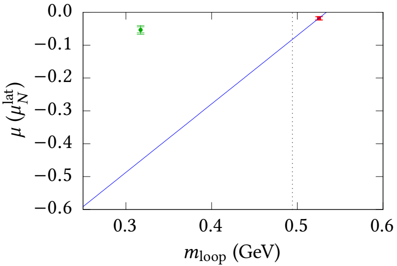


At this order, PQChPT poorly describes the data.
$\longrightarrow$ use simple linear interpolation in $m_{\text{loop}}^2$.

# Strange magnetic moment and radii at physical point

Best estimate at physical quark masses: use linear interpolation in $m^2_{\text{loop}}$:

$$
\begin{aligned}
(r_E^2)^s &= -0.0067(10)(17)(15)\ \text{fm}^2, \\
(r_M^2)^s &= -0.018(6)(5)(5)\ \text{fm}^2, \\
\mu^s &= -0.022(4)(4)(6)\ \mu_N,
\end{aligned}
$$

where the uncertainties are

1. statistical
2. previously estimated systematics
3. physical-point extrapolation
   (= magnitude of shift from result at $m_\pi = 317$ MeV)

# Strange magnetic moment

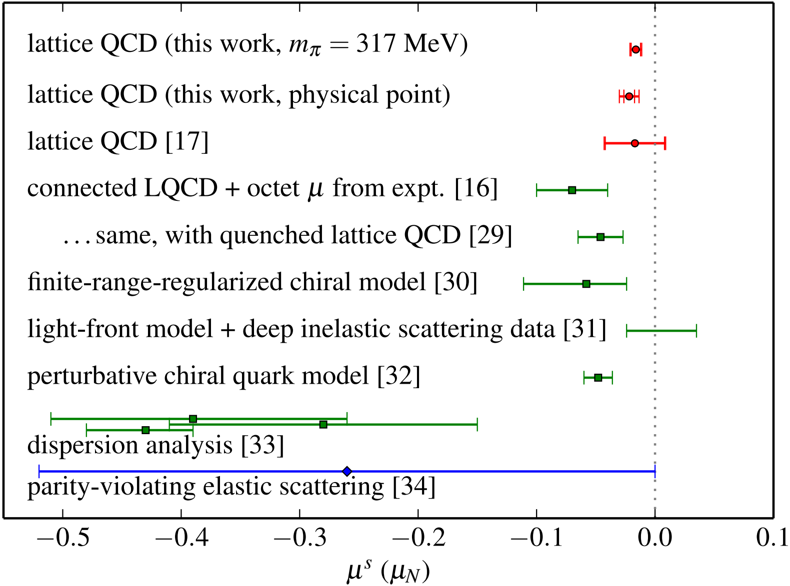

# Contributions to proton electromagnetic obervables

$$(r_E^2)^p = (u, d \text{ contributions}) - \frac{1}{3}(r_E^2)^s \approx (0.88 \text{ fm})^2$$

$$\mu^p = (u, d \text{ contributions}) - \frac{1}{3}\mu^s = 2.793\ldots$$

$$\mu^p(r_M^2)^p = (u, d \text{ contributions}) - \frac{1}{3}(r_M^2)^s \approx 2.793(0.85 \text{ fm})^2$$

In all three cases, the strange-quark contribution is $\sim 0.3$–$0.4\%$.

# Forward-angle scattering experiments

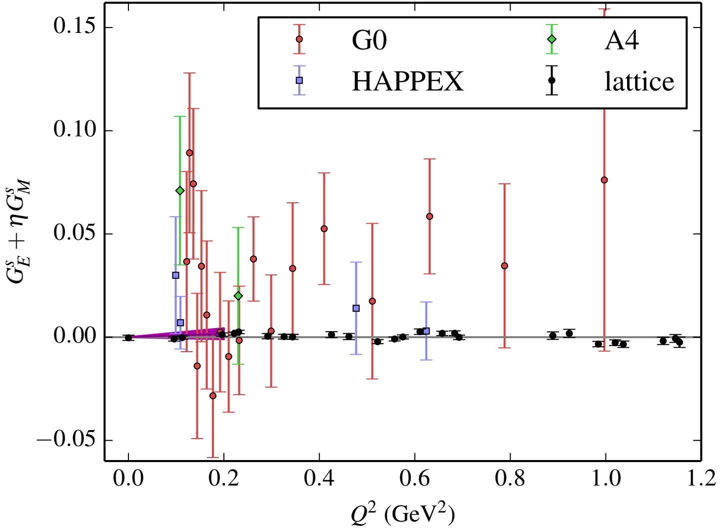


$\eta \approx AQ^2$, $A = 0.94$ GeV$^{-2}$

# Conclusions and outlook

- High statistics and hierarchical probing methods are effective at producing a signal for the disconnected electromagnetic form factors.
- Strange quarks contribute a very small amount to the proton radii and magnetic moment ($\sim 0.3\%$).
- Obtaining a clear nonzero strange-quark signal will be a significant challenge for future parity-violating elastic scattering experiments, especially at forward scattering angles.
- Additional calculations, especially closer to physical quark masses, are needed to confirm the physical-point estimates.
- The same techniques can be applied for other operators, but renormalization is more difficult.